Probing hidden sectors with a muon beam: Implication of spin-0 dark matter mediators for the muon $(g-2)$ anomaly and the validity of the Weiszäcker-Williams approach

H. Sieber,[1,*] D. V. Kirpichnikov,[2] I. V. Voronchikhin,[3] P. Crivelli,[1] S. N. Gninenko,[2] M. M. Kirsanov,[2] N. V. Krasnikov,[2,4] L. Molina-Bueno,[5] and S. K. Sekatskii[6,7]

[1]*ETH Zurich, Institute for Particle Physics and Astrophysics, CH-8093 Zurich, Switzerland*
[2]*Institute for Nuclear Research, 117312 Moscow, Russia*
[3]*Tomsk Polytechnic University, 634050 Tomsk, Russia*
[4]*Joint Institute for Nuclear Research, 141980 Dubna, Russia*
[5]*Instituto de Física Corpuscular, Universidad de Valencia and CSIC, Carrer del Catedrátic José Beltrán Martinez, 2, 46980 Paterna, Valencia, Spain*
[6]*Laboratory of Biological Electron Microscopy, Institute of Physics, Ecole Polytechnique Fédérale de Lausanne, CH-1015 Lausanne, Switzerland*
[7]*Department of Fundamental Microbiology, Faculty of Biology and Medicine, University of Lausanne, BSP 419, 1015 Lausanne, Switzerland*

(Received 24 May 2023; accepted 15 August 2023; published 21 September 2023)

In addition to vector (V) type new particles extensively discussed previously, both CP-even (S) and CP-odd (P) spin-0 dark matter (DM) mediators can couple to muons and be produced in the bremsstrahlung reaction $\mu^- + N \to \mu^- + N + S(P)$. Their possible subsequent invisible decay into a pair of Dirac DM particles, $S(P) \to \chi\bar{\chi}$, can be detected in fixed target experiments through missing energy signature. In this paper, we focus on the case of experiments using high-energy muon beams. For this reason, we derive the differential cross sections involved using the phase space Weiszäcker-Williams approximation and compare them to the exact-tree-level calculations. The formalism derived can be applied in various experiments that could observe muon-spin-0 DM interactions. This can happen in present and future proton beam-dump experiments such as NA62, SHIP, HIKE, and SHADOWS; in muon fixed target experiments as NA64μ, MUonE and M3; in neutrino experiments using powerful proton beams such as DUNE. In particular, we focus on the NA64μ experiment case, which uses a 160 GeV muon beam at the CERN Super Proton Synchrotron accelerator. We compute the derived cross sections, the resulting signal yields and we discuss the experiment projected sensitivity to probe the relic DM parameter space and the $(g-2)_\mu$ anomaly favored region considering 10^{11} and 10^{13} muons on target.

DOI: 10.1103/PhysRevD.108.056018

I. INTRODUCTION

The Standard Model (SM) cannot explain the origin of dark matter (DM), although it makes up almost ≃85% of the Universe's matter [1]. The indirect evidence of DM are associated with the rotational velocities of galaxies, the cosmic structure of a large scale, the anisotropy of the cosmic microwave background, and gravity lensing [2–4]. Nevertheless, the composition of DM continues to be one of the most challenging puzzles for particle physics.

Theoretically, well-motivated scenarios to explain the origin of Dark Matter as a thermal freeze-out relic involve the presence of feebly interacting light scalars from dark sectors (DS) [5,6]. This framework addresses the origin of DM using a similar mechanism to the weakly interacting massive particles and could imply the existence of sub-GeV spin-0 DM mediators with feebly interaction strength [7].

In addition, the observed low energy experimental anomalies such as the recently confirmed tension of 4.2σ [8] in the measurement of the muon's anomalous magnetic moment [9]

$$\Delta a_\mu \equiv a_\mu^{\mathrm{exp}} - a_\mu^{\mathrm{th}} = (251 \pm 59) \times 10^{-11}, \qquad (1)$$

has also motivated the existence of physics beyond the Standard Model and could be explained in DS framework [10]. We note that recent calculations [11–16] of the hadronic vacuum polarization contribution to $(g-2)_\mu$ shifts the anomaly to the level of $\Delta a_\mu = (183 \pm 59) \times 10^{-11}$, that

*Corresponding author: henri.hugo.sieber@cern.ch

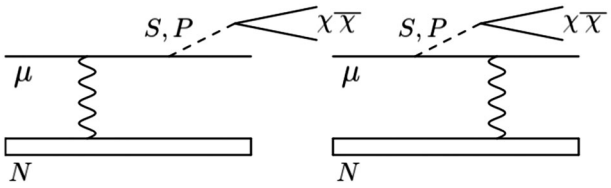

FIG. 1. Diagrams describing spin-0 DM mediator production via bremsstrahlung $\mu N \to \mu N S(P)$, followed by invisible decay $S(P) \to \chi\bar{\chi}$.

corresponds to a significance of 3.1σ [17] (for recent experimental results from CMD-3 collaboration see, e.g., Ref. [18]). In the present paper, we consider the result (1) as a hint of new physics. In particular, a possible solution to that discrepancy involves the introduction of a new weak coupling between the standard matter and a light scalar DM mediator [5,19,20]. Other possibility to address the anomaly considers the case of a light vector mediator (see more details in [21,22]). This study focuses on the computation of the production cross sections of scalar (S) and pseudo-scalar (P) mediators after a high energy muon scatters off in a target (see, e.g., Fig. 1). Our study is particularly relevant to experiments involving high energy muon interactions with a fixed target such as muon experiments NA64μ at CERN [22,23] or the proposal M^3 at Fermilab [19]. Nevertheless, it can also be relevant for (i) current and planned proton beam-dump experiments such as NA62 [24], SHIP [25], HIKE [26], SHADOWS [27], the ILC beam dump [28,29], (ii) muon beam-dump [30], (iii) the MUonE experiment [31], and (iv) DUNE [32] aiming also to perform complementary searches to such hidden particles. In this manuscript, we take as an example the NA64μ experiment at CERN devoted to probe weakly coupled dark sectors with muons.

In the NA64μ experiment, a 160 GeV muon beam is directed to an electromagnetic calorimeter functioning as an active target, where the spin-0 DM mediators are produced. The resulting particles carry away a portion of the primary muon beam energy. The measurement of the primary muon missing momentum is the key feature of the experimental technique.

In this paper, the production cross section of spin-0 particles on the reaction $\mu N \to \mu N S(P)$ are derived. In particular, we show that the widely used Weizsäcker-Williams (WW) approach for the spin-0 production reproduces the exact tree level (ETL) cross sections with an accuracy at the level of $\lesssim \mathcal{O}(5\%)$. Furthermore, a novel analytical formula for computing the differential cross sections in the WW approximation has been obtained in order to perform more accurate and less computationally demanding MC simulations of a dark boson emission. The results have been implemented in the Geant4-based Dark Matter simulation package DMG4 [33,34]. Additionally, we analyze the differential cross sections with respect to the recoil angles of the muon and spin-0 DM mediators relevant to obtain accurate and realistic signal yields in fixed target experiments.

This paper is organized as follows: In Sec. II, we discuss the typical scenarios for spin-0 DM mediators. In Sec. III, we calculate at ETL the total cross section for spin-0 mediator production. In Sec. IV, we discuss the differential cross sections for the angle and energy fraction of the outgoing particles in the WW approach. In Sec. V, we derive novel analytical differential cross sections for the emitted spin-0 mediator in WW approach. In Sec. VI we compare WW and ETL cross sections. Finally, in Sec. VII, we evaluate the projected sensitivities for NA64μ experiment in leptophilic scenarios. We summarize our results and conclusions in Sec. VIII.

II. A SIMPLIFIED MUON-PHILIC MODEL

In this paper, we focus on lepton-specific spin-0 mediators that do not need to couple to neutrinos and assume muon-specific couplings of (pseudo)scalar boson. The simplified muon-philic spin-0 boson Lagrangians can be written for scalar, S, and pseudoscalar, P, respectively as follows

$$\mathcal{L} \supset \mathcal{L}_{\rm SM} + \frac{1}{2}(\partial_\mu S)^2 - \frac{1}{2}m_S^2 S^2 + g_S S\bar{\mu}\mu, \tag{2}$$

$$\mathcal{L} \supset \mathcal{L}_{\rm SM} + \frac{1}{2}(\partial_\mu P)^2 - \frac{1}{2}m_P^2 P^2 + i g_P P\bar{\mu}\gamma_5\mu, \tag{3}$$

where $\mathcal{L}_{\rm SM}$ is the SM Lagrangian, $g_{S(P)}$ is the coupling strength to muons and $m_{S(P)}$ the mass of the mediator. The extension to the dark sector can be introduced through the benchmark couplings to Dirac DM fermions

$$\mathcal{L} \supset \bar{\chi}(i\gamma^\mu\partial_\mu - m_\chi)\chi + g_S^\chi S\bar{\chi}\chi, \tag{4}$$

$$\mathcal{L} \supset \bar{\chi}(i\gamma^\mu\partial_\mu - m_\chi)\chi + i g_P^\chi P\bar{\chi}\gamma_5\chi, \tag{5}$$

where m_χ is a mass of DM particle, g_S^χ and g_P^χ are the typical DM couplings to scalar and pseudoscalar mediators respectively. Moreover, we assume that the invisible decay of $S(P) \to \chi\bar{\chi}$ will be the dominant channel. This means that we focus only on the benchmark regime $m_{S(P)} \gtrsim 2m_\chi$ and $g_{S(P)}^\chi \gg g_{S(P)}$ in the present study.

We also note that scalar couplings (2) can be originated from flavor specific Lagrangian of higher dimensions in Higgs extended sectors [35] that can be probed by accelerator-based experiments [5,19,20]. For pseudoscalar benchmark couplings (3) we address the reader to Ref. [36], where muon-specific ALPs signatures were studied in detail in the light of atmospheric probes of ALPs using Cerenkov detectors near the Earth's surface.

The one-loop leading order contributions from scalars to the $(g-2)_\mu$ are obtained through the Yukawa-like interaction and are given by [37–40]

$$\Delta a_S = \frac{g_S^2}{8\pi^2}\int_0^1 dx \frac{m_\mu^2(1-x)(1-x^2)}{m_\mu^2(1-x)^2 + m_S^2 x}, \tag{6}$$

where we defined $g_S = e\epsilon_S$, with $e = \sqrt{4\pi\alpha}$ the electric charge and $\alpha \simeq 1/137$ the fine-structure constant. In the case where $m_S/m_\mu \to 0$, $g_S = (3.63 \pm 0.43) \times 10^{-4}$.

On the other side, the one-loop contribution of the muon-philic pseudoscalar boson to Δa_μ is negative, so the CP-odd spin-0 mediator cannot accommodate the explanation of the $(g-2)_\mu$ anomaly [36]. For completeness, we refer the reader to [21] for a discussion of the contribution of the vector-boson. In addition, for recent progress on probing leptophilic dark sector see also Refs. [25,41–43].

III. THE EXACT TREE-LEVEL CALCULATION

In the following, we discuss the computations of the exact-tree-level production cross sections for both, a light scalar and pseudoscalar muon-philic boson. We follow the notations of [44,45]. We refer to the kinematic variables of the process $\mu^-(p) + N(P_i) \to \mu^-(p') + N(P_f) + H(k)$ from our previous work [21]. Here we denote via $H = (S, P)$ the general muon-specific CP-even and CP-odd spin-0 boson. Let us recall the definition of the double-differential cross section [44]

$$\left.\frac{d\sigma}{dx d\cos\theta_H}\right|_{\rm ETL} = \frac{\epsilon_H^2\alpha^3|\mathbf{k}|E_\mu}{|\mathbf{p}||\mathbf{k}-\mathbf{p}|}\int_{t_{\rm min}}^{t_{\rm max}}\frac{dt}{t^2}G_2^{el}(t)\int_0^{2\pi}\frac{d\phi_q}{2\pi}\frac{|\mathcal{A}^H_{2\to3}|^2}{8M^2}, \tag{7}$$

where $x = E_H/E_\mu$ is a fractional energy, $t_{\rm min}$ and $t_{\rm max}$ the minimum and maximum momenta transfer and $G_2^{el}(t)$ the squared elastic form factor as defined in [21,44,46], ϕ_q is the axial angle of the three momentum transfer to the nucleus $\boldsymbol{q} = \boldsymbol{P}_i - \boldsymbol{P}_f$ defined in the polar frame in Ref. [44]. The amplitude squared associated to the production of a (pseudo) scalar boson is calculated using the FeynCalc package [47] embedded in the Wolfram- language-based *Mathematica* package [48]. With similar kinematics as defined for the vector V–boson, we obtain in the case $H = S$

$$\begin{aligned}|\mathcal{A}^S_{2\to3}|^2 = \frac{1}{\tilde{u}^2\tilde{s}^2}\{&4(4m_\mu^2 - m_S^2)(\mathcal{P}\cdot p')^2\tilde{s}^2 - 4[t(\mathcal{P}\cdot p)^2\\ &- 2(4m_\mu^2 - m_S^2 + t)(\mathcal{P}\cdot p)(\mathcal{P}\cdot p')\\ &+ t(\mathcal{P}\cdot p')^2]\tilde{s}\tilde{u} + 4(4m_\mu^2 - m_S^2)(\mathcal{P}\cdot p)^2\tilde{u}^2\\ &+ \mathcal{P}^2[\tilde{s}+\tilde{u}]^2[(m_S^2 - 4m_\mu^2)t + \tilde{s}\tilde{u}]\},\end{aligned} \tag{8}$$

as well as for the pseudoscalar particle, $H = P$,

$$\begin{aligned}|\mathcal{A}^P_{2\to3}|^2 = \frac{1}{\tilde{u}^2\tilde{s}^2}\{&8(-m_P^2 + t)(\mathcal{P}\cdot p)(\mathcal{P}\cdot p')\tilde{s}\tilde{u}\\ &- 4(\mathcal{P}\cdot p)^2\tilde{u}(t\tilde{s} + m_P^2\tilde{u}) - 4(\mathcal{P}\cdot p')^2\tilde{s}(t\tilde{u} + m_P^2\tilde{s})\\ &+ \mathcal{P}^2(\tilde{s}+\tilde{u})^2(m_P^2 t + \tilde{s}\tilde{u})\},\end{aligned} \tag{9}$$

for which the relevant Mandelstam variables and dot products read

$$\begin{aligned}\tilde{s} &= (p'+k)^2 - m_\mu^2 = 2(p'\cdot k) + m_H^2,\\ \tilde{u} &= (p-k)^2 - m_\mu^2 = 2(p\cdot k) + m_H^2,\end{aligned} \tag{10}$$

$$\mathcal{P}^2 = 4M^2 + t(p'+k)^2, \quad (\mathcal{P}\cdot p) = 2ME_\mu - (\tilde{s}+t)/2, \tag{11}$$

$$\mathcal{P}\cdot p' = 2M(E_\mu - E_H) + (\tilde{u} - t)/2, \tag{12}$$

with $\mathcal{P}_\mu = (P_i + P_f)_\mu$, $P_i = (M, 0)$ being the nucleus four-momentum in the laboratory frame, $P_f = (P_f^0, \mathbf{P}_f)$ is its outgoing momentum. The resulting squared matrix elements Eqs. (8) and (9) coincide with those given in Refs. [44,46], implying replacement of the electron with muon, i.e. $m_e \to m_\mu$.

IV. THE WW APPROXIMATIONS FOR THE (PSEUDO)SCALAR EMISSION CROSS SECTIONS

In this section, we use the Weizsäcker-Williams (WW) approximation to compute the double-differential production cross sections for H, assuming that the energy of the incoming muon is much larger than both m_μ and m_H. In this approach, the flux of virtual photons from the moving charged particles can be treated as a plane wave and approximated by real photons. We follow the same procedure as the one described in [21], Sec. III, namely considering the effective photon flux to read

$$\chi = \int_{t_{\rm min}}^{t_{\rm max}} dt\,\frac{t - t_{\rm min}}{t^2}F^2(t), \tag{13}$$

where $t_{\rm min} \simeq U^2(x,\theta_H)/(4E_\mu^2(1-x)^2)$ and $t_{\rm max} = m_H^2 + m_\mu^2$ are the minimum and maximum momentum transfer to the nuclei. The function U^2 is given by Eq. (19) below and depends on the fractional energy $x = E_H/E_\mu$ and the H–boson recoil angle θ_H. $F^2(t)$ is the squared elastic form factor, whose exact form is given in [21]. In particular, for the choice of (x,θ_H) and (y,ψ_μ) variables, the WW-approximated quantities read respectively

$$\left.\frac{d\sigma^H_{2\to3}}{dx d\cos\theta_H}\right|_{\rm WW} \simeq \frac{\alpha\chi}{\pi(1-x)}E_\mu^2 x\beta_H\left.\frac{d\sigma^H_{2\to2}}{d(pk)}\right|_{t=t_{\rm min}}, \tag{14}$$

$$\left.\frac{d\sigma^H_{2\to3}}{dy d\cos\psi_\mu}\right|_{\rm WW} \simeq \frac{\alpha\chi}{\pi(1-y)}E_\mu^2 y\beta_{\mu'}\left.\frac{d\sigma^H_{2\to2}}{d(pk)}\right|_{t=t_{\rm min}}, \tag{15}$$

where $\beta_H = (1 - m_H^2/(xE_\mu)^2)^{1/2}$ is the typical velocity of the produced hidden boson, $\beta_\mu = (1 - m_\mu^2/(yE_\mu)^2)^{1/2}$ and $y = E_{\mu'}/E_\mu$ are the typical velocity of the recoil muon and its energy fraction respectively, ψ_μ the recoil angle of outgoing muon. The expression of the photon flux χ is given by (13). The cross section of the process $\mu\gamma \to \mu H$ has the following form

$$\frac{d\sigma^H_{2\to 2}}{d(pk)} = \epsilon_H^2\alpha^2\frac{2\pi}{\tilde{s}^2}|\mathcal{A}^H_{2\to 2}|^2, \tag{16}$$

where the squared amplitudes read

$$|\mathcal{A}^S_{2\to 2}|^2 = 2(m_S^2 - 4m_\mu^2)\left[\left(\frac{\tilde{s}+\tilde{u}}{\tilde{s}\,\tilde{u}}\right)^2 m_\mu^2 - \frac{t_2}{\tilde{s}\,\tilde{u}}\right] - \frac{(\tilde{s}+\tilde{u})^2}{\tilde{s}\,\tilde{u}}, \tag{17}$$

$$|\mathcal{A}^P_{2\to 2}|^2 = 2m_P^2\left[\left(\frac{\tilde{s}+\tilde{u}}{\tilde{s}\,\tilde{u}}\right)^2 m_\mu^2 - \frac{t_2}{\tilde{s}\,\tilde{u}}\right] - \frac{(\tilde{s}+\tilde{u})^2}{\tilde{s}\,\tilde{u}}. \tag{18}$$

We note that for the (x,θ_H)—plane one has the following expressions for the Mandelstam variables

$$\tilde{s} \simeq U/(1-x), \qquad U = E_\mu^2\theta_H^2 x + m_H^2(1-x)/x + m_\mu^2 x, \tag{19}$$

$$\tilde{u} \simeq -U, \qquad t_2 = -xU/(1-x) + m_H^2. \tag{20}$$

On the other hand, for the (y,ψ_μ)—plane the Mandelstam variables read

$$\tilde{s} \simeq \tilde{t}/(1-y), \quad \tilde{u} \simeq -y\tilde{t}/(1-y), \quad \tilde{t} \simeq m_H^2 - t_2, \tag{21}$$

$$t_2 \simeq -[E_\mu^2\psi_\mu^2 y + m_\mu^2(1-y)/y + m_\mu^2 y] + m_\mu^2. \tag{22}$$

Here we assume that the photon virtuality is sufficiently small $t \equiv -q^2 \ll \tilde{s}, \tilde{u}, t_2$. Thus we neglect q^2 in Eqs. (17) and (18) implying that the longitudinal part of the amplitude squared $2\to 2$ is small compared to the transverse term (see, e.g., Ref. [49]). Let us also remark on the typical energy fractions of the outgoing muon and H boson in the process $\mu N \to \mu N H$ for certain benchmark kinematics. The lowest possible energy of the produced H-boson implies that $x_{\min} \simeq m_H/E_\mu \lesssim x$, i.e., in this case the spin-0 particle is produced with zero three-momentum, $|\mathbf{k}| = 0$. This means also that almost all energy of the initial muon is transferred to the outgoing muon, which leads to the typical bound $y \lesssim y_{\max} \simeq 1 - m_H/E_\mu$. On the other hand, if the initial muon transfers its maximal energy to spin-0 boson, then we get $y \gtrsim y_{\min} \simeq m_\mu/E_\mu$ and $x \lesssim x_{\max} \simeq 1 - m_\mu/E_\mu$.

V. ANALYTICAL INTEGRATION OF THE WW APPROXIMATION OVER THE ANGLE θ_H

In the WW approach, the lower bound of the flux integral $t_{\min}$ depends on both the fractional energy x and the emitted angle θ_H of the boson mediator. Although WW provides more accurate results than its improved approach (IWW), the integration of the double-differential cross section is still computationally expensive, to sample a sufficiently large number of MC events [33]. In this work, we perform an explicit integration over θ_H to obtain an analytical expression for $d\sigma^H_{2\to 3}/dx$. We emphasize that this result can also be expanded to the light V vector boson case.

The formula for the differential cross section can be rewritten in the following form

$$\left.\frac{d\sigma^H_{2\to 3}}{dx}\right|_{\rm WW} = \epsilon_H^2\alpha^3\sqrt{x^2 - \frac{m_H^2}{E_\mu^2}}\frac{1-x}{x}\int_{u_{\min}}^{u_{\max}} du\frac{|\mathcal{A}^H_{2\to 2}|^2\chi}{u^2}, \tag{23}$$

where the limits of integration over the Mandelstam variable are

$$u_{\max} = -m_H^2(1-x)/x - m_\mu^2 x, \tag{24}$$

$$u_{\min} = -xE_\mu^2(\theta_H^{\max})^2 - m_H^2(1-x)/x - m_\mu^2 x, \tag{25}$$

where $\theta_H^{\max}$ is the typical maximal angle between the initial muon and the emission momentum of the H boson. Numerical analysis show (see e. g. Sec. VI below) that for the ultrarelativistic muons expected at NA64μ one can set $\theta_H^{\max} \simeq 0.1$. It is worth noticing that in Eq. (23) we imply $d\cos\theta_H \simeq du/(2xE_\mu^2)$ in order to introduce a new variable of the integration u instead of $\cos\theta_H$. The transition amplitude squared then reads

$$|\mathcal{A}^H_{2\to 2}|^2(x,u) = C_1^H + C_2^H\frac{1}{u} + C_3^H\frac{1}{u^2}, \tag{26}$$

where the coefficients C_i^H are

$$C_1^S = C_1^P = \frac{x^2}{1-x}, \qquad C_2^S = 2(m_S^2 - 4m_\mu^2)x, \tag{27}$$

$$C_2^P = 2m_P^2 x, \qquad C_3^P = 2m_P^2(m_P^2(1-x) + m_\mu^2 x^2), \tag{28}$$

$$C_3^S = 2(m_S^2 - 4m_\mu^2)(m_S^2(1-x) + m_\mu^2 x^2). \tag{29}$$

For completeness, we also derive the coefficients for the vector boson emission. In particular, for the case of $H = V$ these quantities read explicitly in the following form

$$C_1^V = 2\frac{(2-2x+x^2)}{1-x}, \qquad C_2^V = 4(m_V^2 + 2m_\mu^2)x, \tag{30}$$

$$C_3^V = 4(m_V^2 + 2m_\mu^2)(m_V^2(1-x) + m_\mu^2 x^2). \tag{31}$$

The flux of virtual photons χ in the Weizsacker-Williams approximation can be expressed via the typical elastic atomic form-factor in the following form

$$\chi = Z^2\int_{t_{\min}}^{t_{\max}}\frac{t-t_{\min}}{t^2}\left(\frac{t}{t_a+t}\right)^2\left(\frac{t_d}{t_d+t}\right)^2 dt = C_1^\chi + C_2^\chi u^2 + C_3^\chi\ln\left(\frac{u^2g^2+t_d}{u^2g^2+t_a}\right) + C_4^\chi u^2\ln\left(\frac{u^2g^2+t_d}{u^2g^2+t_a}\right), \tag{32}$$

where $Z = 82$ is the atomic number of the lead target of NA64μ, $\sqrt{t_a} = 1/R_a$ is a momentum transfer associated

with nucleus Coulomb field screening due to the atomic electrons, with R_a being a typical magnitude of the atomic radius $R_a = 111Z^{-1/3}/m_e$, $\sqrt{t_d} = 1/R_n$ is the typical momentum associated with nuclear radius R_n, such that $R_n \simeq 1/\sqrt{d}$ and $d = 0.164A^{-2/3}$ GeV^2, $A = 207$ is the atomic mass number of the lead target, $t_{\min} = g^2u^2$ is minimal transfer momentum, here we denote $g = 1/(2E_\mu(1-x))$ for simplicity. Typically the maximal transfer momentum $t_{\max}$ is chosen to be $t_{\max} = m_\mu^2 + m_H^2$ in [44,46], however, the numerical calculations reveal that $t_{\max}$ can be set as large as $t_{\max} \gtrsim t_d$ in order to achieve a better accuracy for WW approach. The coefficients $C_1^\chi, C_2^\chi, C_a^\chi$, and C_4^χ in (32) are collected in Appendix.

By substituting Eqs. (32) and (26) into the differential cross section (23) one can obtain the following expression:

$$\left(\frac{d\sigma}{dx}\right)_{\rm WW} = \epsilon_H^2\alpha^3\sqrt{x^2 - \frac{m_H^2}{E_\mu^2}}\frac{1-x}{x}\int_{u_{\min}}^{u_{\max}}\left\{C_1^H C_2^\chi + \frac{C_2^H C_2^\chi}{u} + \frac{C_1^H C_1^\chi + C_3^H C_2^\chi}{u^2} + \frac{C_2^H C_1^\chi}{u^3} + \frac{C_3^H C_1^\chi}{u^4} + \left[C_1^H C_4^\chi + \frac{C_2^H C_4^\chi}{u} + \frac{C_1^H C_3^\chi + C_3^H C_4^\chi}{u^2} + \frac{C_2^H C_3^\chi}{u^3} + \frac{C_3^H C_3^\chi}{u^4}\right]\ln\left(\frac{u^2g^2 + t_d}{u^2g^2 + t_a}\right)\right\}du. \quad (33)$$

The differential cross section with respect to x, can be represented as the sum of six typical terms

$$\left(\frac{d\sigma}{dx}\right)_{\rm WW} = \epsilon_H^2\alpha^3\sqrt{x^2 - \frac{m_H^2}{E_\mu^2}}\frac{1-x}{x}\sum_{i=1}^{6}\Delta I_i^H(x,u), \quad (34)$$

where $\Delta I_i^H(x,u) = I_i^H(x,u_{\max}) - I_i^H(x,u_{\min})$. The functions $I_i^H(x,u)$ are described in Appendix. Alternatively, one can also exploit the state-of-the-art MadGraph [50] or CalcHEP [51] packages with appropriate atomic form-factor implementation [20,42,52–56]. That analysis, however, is beyond the scope of the present paper.

VI. NUMERICAL INTEGRATION OF THE CROSS SECTIONS

The comparison between the expression for $d\sigma/dxd\cos\theta_H$ at ETL and in the WW approximation is shown for both scalar and pseudoscalar mediators in Figs. 2 and 3. The H mass spans from 10 MeV to 1 GeV. Following the nominal beam energy of the NA64μ experiment, the initial state muon energy is set to $E_\mu = 160$ GeV. The integration over (t, ϕ_q) in Eq. (7) is performed using the parametrization of [57] to integrate out ϕ_q. The integral over t is computed numerically through Monte Carlo integration [58]. Only the region of phase space (x, θ_H) where the double-differential cross section contributes more is shown. Both the complete calculation (ETL) and the WW results have the double differential cross section peak at the same order of magnitude. Additionally, from both Figs. 2 and 3 it can be seen that θ_H is constant around $\sim 5 \times 10^{-4}$ as expected from the typical emission angle

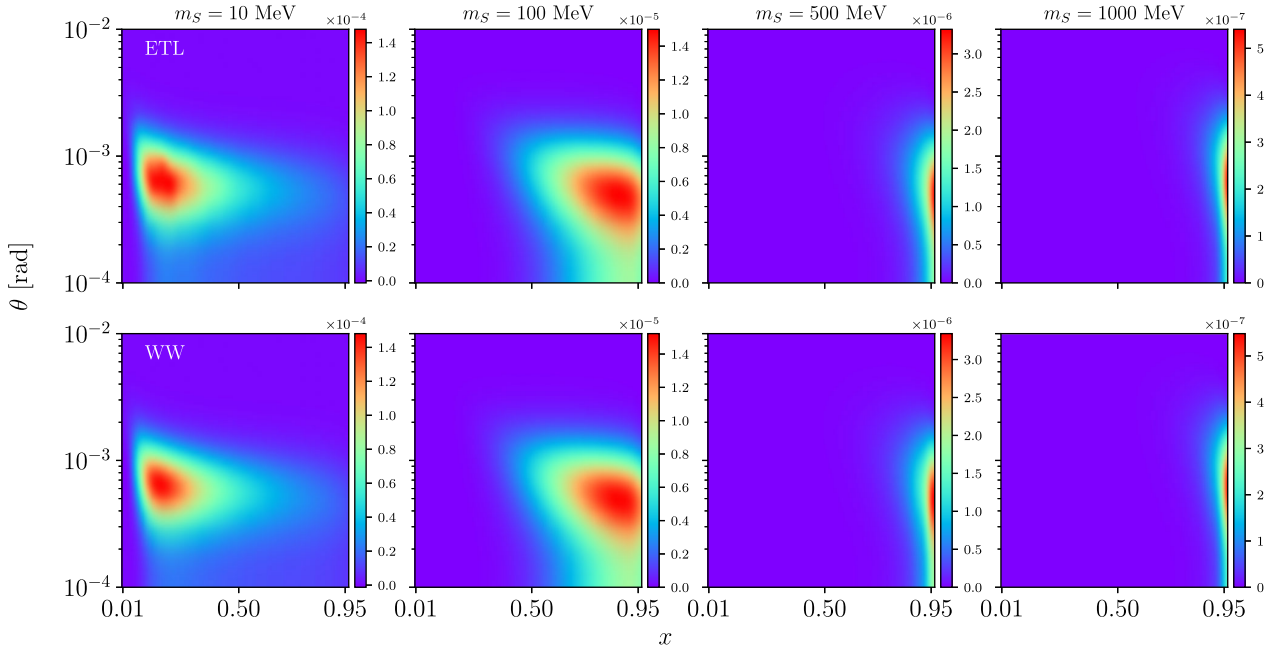

FIG. 2. Top: double-differential cross section at ETL in the (x, θ_S) space. The expression of Eq. (7) is integrated using both the angular parametrization from [57] and MC integration [58]. Bottom: double-differential cross section in the WW approach for the (x, θ_S) variables [see Eq. (14) with an amplitude squared as defined in Eq. (17)]. The mass range spans from 10 MeV to 1 GeV. The mixing strength is $\epsilon_S = 10^{-4}$.

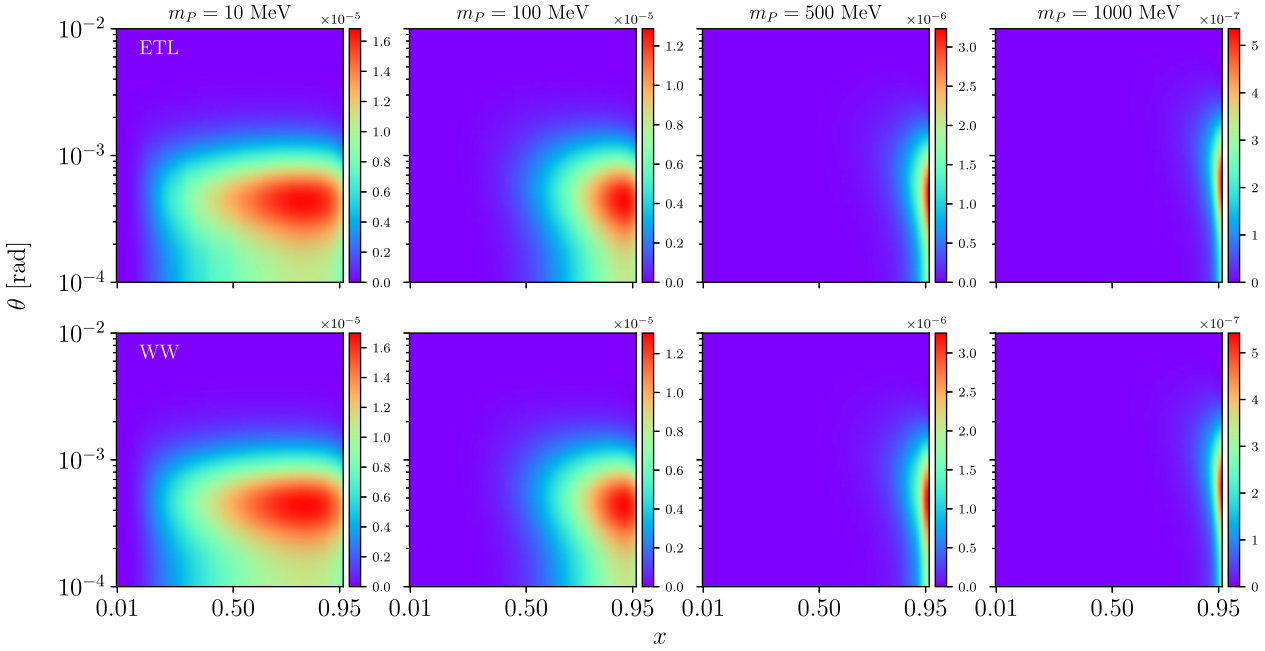

FIG. 3. The same as in Fig. 2 but for pseudoscalar field P.

$\sim m_\mu/E_\mu$, which is independent of m_H. To perform the comparison between the ETL and WW approximated results, Eq. (7) is integrated over θ and compared to the expression in Eq. (34). The results in the case $H = S$ and $H = P$ are shown respectively in Figs. 4 and 5. In both cases the integrated differential cross section relative error with respect to the exact calculation is below $\lesssim\mathcal{O}(5\%)$ for the full mass range.

However, on the boundaries of the fractional energy domain, $x \to x_{\min} \ll 1$ and $x \to x_{\max} \simeq 1$, the relative error can be as large as $\gtrsim\mathcal{O}(5\%)$. After the numerical integration of the differential cross section, this effect is negligible. Therefore, the yields of the produced spin-0 bosons can be calculated accurately in WW approach [21].

For completeness, the single differential cross sections with respect to the outgoing muon fractional energy, y, and emission angle, ψ, are integrated according to Eq. (15). The results are illustrated in Figs. 6 and 7. Similarly as in the result for the integration over x, the integrated differential cross section relative error is of the order $\lesssim\mathcal{O}(5\%)$.

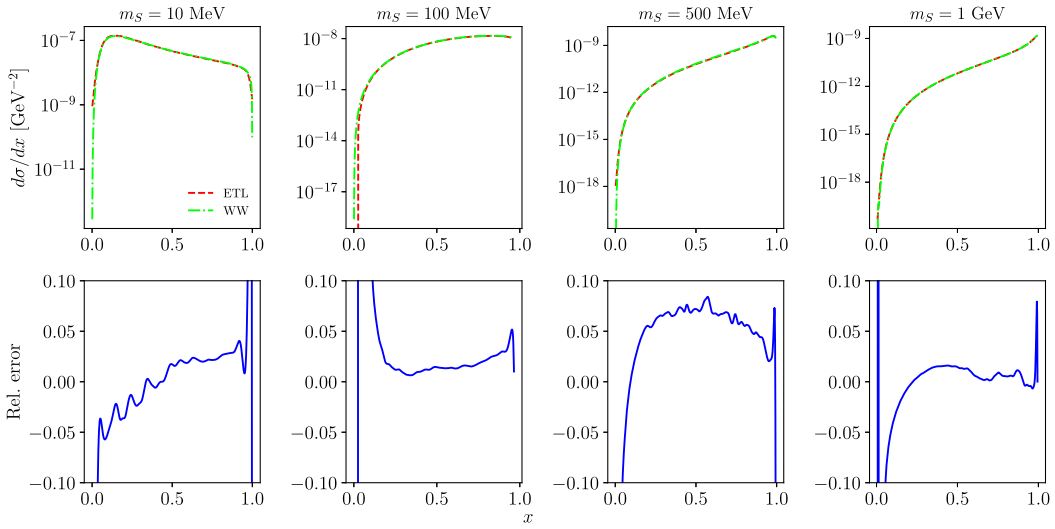

FIG. 4. Top: single-differential scalar mediator cross sections as a function of x in the ETL (red dashed line) and WW approximation (green dashed line) regime for different mass values. The exact approach (ETL) results are obtained numerically through integration by quadrature of the results of Fig. 2. Bottom: relative error, $(\mathcal{O}_{\rm WW} - \mathcal{O}_{\rm ETL})/\mathcal{O}_{\rm ETL}$, between the WW and ETL expressions defined respectively in Eqs. (7) and (34). The mixing strength is $\epsilon_S = 10^{-4}$.

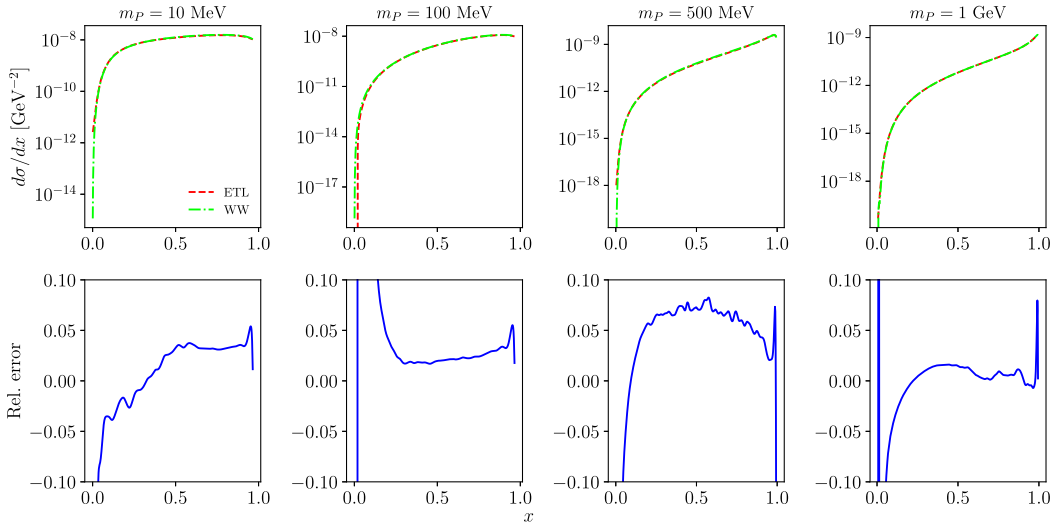

FIG. 5. The same as in Fig. 4 but for pseudoscalar mediator P.

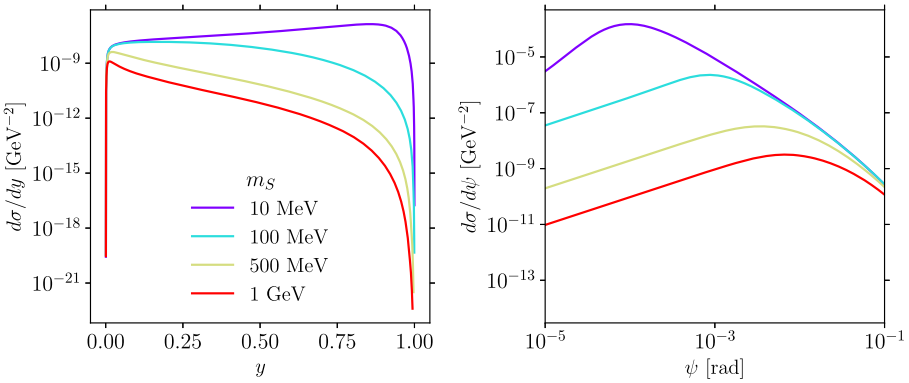

FIG. 6. Single-differential scalar mediator cross sections in WW approximation regime for different mass values (from the top to the bottom line the masses are 10, 100, 500, and 1000 MeV). The mixing strength is $\epsilon_S = 10^{-4}$. Left: single-differential cross section as a function of the outgoing muon fractional energy. Right: single-differential cross section as a function of the outgoing muon angle.

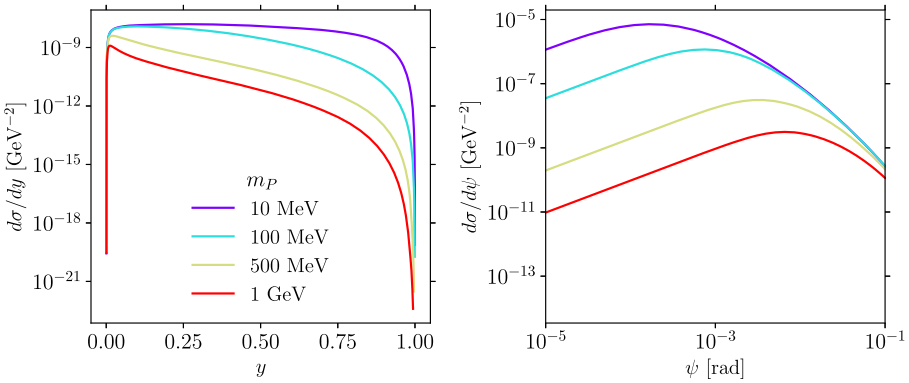

FIG. 7. The same as in Fig. 6 but for pseudoscalar mediator P.

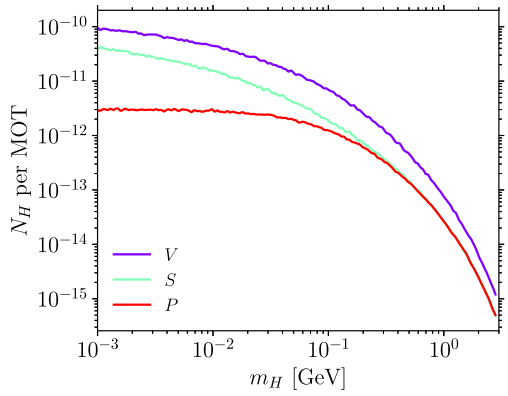

FIG. 8. Number of light mediators, N_H, per muons on target (MOT) as obtained through a full Geant4 simulation of the NA64μ target using the DMG4 package ($\epsilon_H = 10^{-4}$ is considered in this case). For completeness, in addition to the scalar (S) and pseudoscalar (P) mediators is also shown the vector (V) case.

VII. PROJECTED SENSITIVITIES TO THE MIXING STRENGTH

The typical estimate of the sensitivity of a given experiment can be computed following the yield formula [45]

$$N_H = N_{\mathrm{MOT}} \frac{\rho \mathcal{N}_A}{A} \sum_i \sigma_H(E_i) \Delta L_i, \tag{35}$$

where ρ and A are respectively the target density and its atomic weight, E_i the energy of the muon at the ith step-length ΔL_i in the target and N_{MOT} the number of muons on target. We recall that NA64μ target is a lead-scintillator sandwich electromagnetic calorimeter of 40 radiation lengths ($40X_0$) [22]. However, for a realistic sensitivity study of one's experiment to new physics models, including particles propagation through the detectors, the differential cross sections for the production of light muon-philic mediators are implemented using the interface provided by the fully Geant4 [59] compatible DMG4 package. In Fig. 8 the production yields for both cases $H = S$ and $H = P$ as obtained through a realistic Geant4 simulation of the NA64μ detectors are shown. The number of signal events N_H are given in the scenario where $\epsilon_H = 10^{-4}$. For completeness, the yield for the vector case ($H = V$), for which the similar calculations and implementation were performed previously, is plotted.

The sensitivity of the experiment in the case where $H = S$ and $H = P$ is shown in Fig. 9 in the invisible scenario, $S \to$ invis, in the target parameter space (m_H, g_H). Equation (34) is considered, i.e., the WW regime, and embedded in the aforementioned simulation framework. The limits are calculated at 90% C. L., requiring $N_H \gtrsim 2.3$, and assuming 100% efficiency and no background. It is worth noting that our work provides a better precision of the signal yield than in Ref. [5] where the projected limits are obtained through pure numerical integration of the production cross section in the improved WW (IWW) approach for which the relative error can be as large as 40% [21]. In the chosen mass range, both sensitivities for the case $H = S$ and $H = P$ yield similar reach as Eqs. (17) and (18) only differ by the typical factors $m_S^2 - 4m_\mu^2$ and m_P^2.

NA64μ projected sensitivity for 10^{13} MOT can completely probe the new physics contribution to the $(g-2)_\mu$ anomaly for a muon-philic scalar mediator for masses below 3 GeV. The DM relic predictions have been obtained in [5]. The "kink" present in the DM relic curves arises as at $m_S = 2m_\mu$ a new annihilation channel to muons is kinematically accessible. For a similar mass range and MOT,

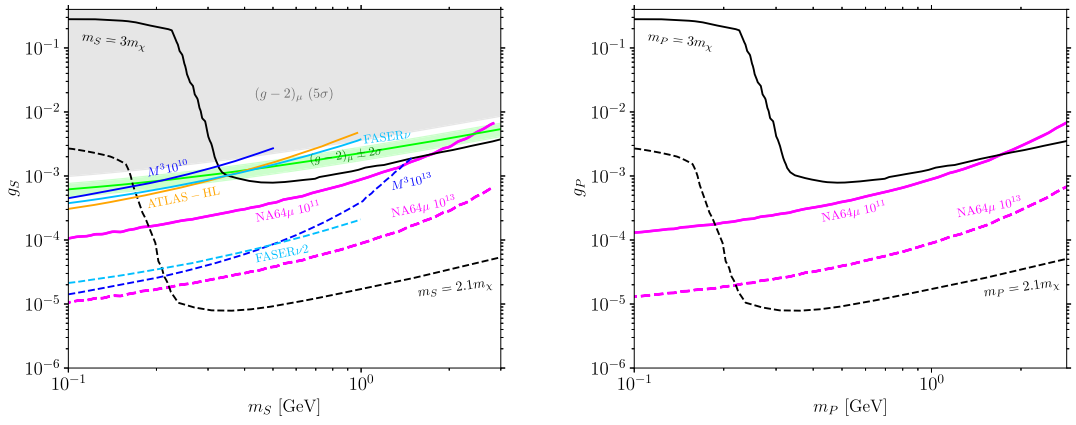

FIG. 9. Projected sensitivity in the (m_H, g_μ) phase space obtained through a full Geant4-based [59] Monte Carlo simulations of the NA64μ set-up, together with the embedding of Eq. (34) in the DMG4 package [33] for 10^{11} (plain magenta line) and 10^{13} (dashed magenta line) MOT. The limits are calculated at 90% C.L. Left: scalar (S) case. Are also shown the $(g-2)_\mu \pm 2\sigma$ band following Eq. (6) and the thermal freeze-out target as computed in [5] for the scenario $g_\chi = 1$ both with $m_S = 3m_\chi$ and $m_S \simeq 2.1m_\chi$. The M^3 experiment phases 1 and 2 (plain and dashed blue lines) are shown for completeness [19] together with the ATLAS HL-LHC analysis at $\mathcal{L}_{\mathrm{LHC}} = 3\ \mathrm{ab}^{-1}$ [60] (orange line) and the FASERν projected sensitivity at $\mathcal{L}_{\mathrm{LHC}} = 250\ \mathrm{fb}^{-1}$ (light blue line) and $\mathcal{L}_{\mathrm{LHC}} = 3\ \mathrm{ab}^{-1}$ (dashed light blue line) [56]. Right: pseudoscalar (P) case.

the target parameter space for thermal relic DM with a scalar mediator is fully accessible in the scenario where $g_S^\chi = 1$ and $m_S = 3m_\chi$. Because of the similar behavior of the cross sections at masses above the muon mass ($m_S \gtrsim m_\mu$), the previous statement is also valid in the case of a pseudoscalar mediator, $H = P$. In the near-resonant scenario for which $m_S \simeq 2.1 m_\chi$, only the portion of parameter space with $m_H \lesssim \mathcal{O}(m_\mu)$ is accessible. Note that for completeness projected sensitivities from both M^3 phases I and II are shown for 10^{10} MOT and 10^{13} MOT respectively given the phase-space values provided in [19]. Additionally, the ATLAS-HL [60] and FASERν(2) [56] expected limits are shown.

VIII. SUMMARY

In this work, we have derived, based on the work of [21,44,46], the differential cross sections for spin-0 DM mediator production in fixed target experiments through muon bremsstrahlung. We have shown that the commonly used Weiszäcker-Williams approximation reproduces well the exact-tree-level calculations cross section with an accuracy at the level of $\lesssim\mathcal{O}(5\%)$ in the high-energy beam regime. We have also calculated the $S(P)$ differential cross section as a function of new variables, namely the scattered muon fractional energy and recoil angle, of potential importance for Monte Carlo simulations and in the estimate of realistic signal yields in missing momentum experiments. Additionally, we developed an analytical expression of the differential cross section of spin-0 mediators in WW approximation to reduce computational time due to numerical integration. We highlight that the results derived can be relevant for different experiments such as proton beam-dump as NA62, SHADOWS, SHIP and HIKE, muon fixed target experiments such as NA64μ, MUonE and M3, and future neutrino experiments as DUNE. In this work, we have considered as benchmark the NA64μ experiment. Finally, our calculations were used to derive the projected sensitivities of the experiment to probe leptophilic scenarios. Our results demonstrate the potential of muon fixed target experiments to explore a broad coupling and mass region parameter space of spin-0 DM mediators, including the DM relic and the $(g-2)_\mu$ anomaly favored parameter space.

ACKNOWLEDGMENTS

We acknowledge the members of the NA64 collaboration for fruitful discussions. D. K. and I. V. are indebted to R. Dusaev, D. Forbes, Y. Kahn, V. Lyubovitskij, A. Pukhov, and A. Zhevlakov for helpful suggestions and correspondence. The work of D. V. K. on calculation of spin-0 mediator emission is supported by the Russian Science Foundation RSF Grant No. 21-12-00379. The work of P. C. and H S. is supported by SNSF and ETH Zurich Grants No. 186181, No. 186158 and No. 197346 (Switzerland). The work of L. M.-B. is supported by SNSF Grant No. 186158 (Switzerland), RyC-030551-I, and PID2021-123955NA-100 funded by MCIN/AEI/10.13039/501100011033/FEDER, UE (Spain).

APPENDIX: SPECIAL FUNCTIONS

In this section, we collect the coefficients needed for the analytical differential cross section calculation

$$C_1^\chi = \frac{Z^2 t_d^2}{(t_a - t_d)^3}\left(\frac{t_d(t_a-t_d)}{t_d+t_{\max}} + \frac{t_a(t_a-t_d)}{t_a+t_{\max}} - -2(t_a-t_d) + (t_a+t_d)\ln\left(\frac{t_d+t_{\max}}{t_a+t_{\max}}\right)\right),$$

$$C_2^\chi = \frac{Z^2 t_d^2 g^2}{(t_a-t_d)^3}\left(\frac{t_a-t_d}{t_d+t_{\max}} + \frac{t_a-t_d}{t_a+t_{\max}} + 2\ln\left(\frac{t_d+t_{\max}}{t_a+t_{\max}}\right)\right),$$

$$C_3^\chi = -\frac{Z^2 t_d^2 (t_a+t_d)}{(t_a-t_d)^3}, \qquad C_4^\chi = -\frac{2Z^2 t_d^2 g^2}{(t_a-t_d)^3}.$$

The coefficients for the resulting cross section (34) are

$$I_1^H(x,u) = C_1^H C_2^\chi u + C_2^H C_2^\chi \frac{\ln(u^2)}{2} - \frac{C_1^H C_1^\chi + C_3^H C_2^\chi}{u} - \frac{C_2^H C_1^\chi}{2u^2} - \frac{C_3^H C_1^\chi}{3u^3}, \tag{A1}$$

$$I_2^H(x,u) = \frac{C_3^H C_3^\chi}{3} \cdot \left\{-\frac{1}{u^3} f_1(x,u) - 2\frac{g^2}{u}\left(\frac{1}{t_d} - \frac{1}{t_a}\right) - f_2(x,u,4)\right\}, \tag{A2}$$

$$I_3^H(x,u) = \frac{C_2^H C_3^\chi}{2}\left\{f_3(x,u) - \frac{1}{u^2} f_1(x,u)\right\}, \tag{A3}$$

$$I_4^H(x,u) = (C_1^H C_3^\chi + C_3^H C_4^\chi)\left\{f_2(x,u,2) - \frac{1}{u} f_1(x,u)\right\}, \tag{A4}$$

$$I_5^H(x,u) = \frac{C_2^H C_4^\chi}{2} \cdot \left\{\ln\left(\frac{t_d}{t_a}\right)\ln(u^2) - Li_2\left(-\frac{g^2u^2}{t_d}\right) + Li_2\left(-\frac{g^2u^2}{t_a}\right)\right\}, \tag{A5}$$

$$I_6^H(x,u) = C_1^H C_4^\chi \{u f_1(x,u) + f_2(x,u,0)\}, \tag{A6}$$

where $Li_2(x)$ is a polylogarithm and the auxiliary functions are

$$f_1(x,u) = \ln\left(\frac{u^2+b}{u^2+a}\right), \qquad b = \frac{t_d}{g^2}, \qquad a = \frac{t_a}{g^2}, \tag{A7}$$

$$f_2(x,u,n) = 2\left(\frac{1}{b}\right)^{\frac{n-1}{2}} \arctan\left(\frac{u}{\sqrt{b}}\right) - 2\left(\frac{1}{a}\right)^{\frac{n-1}{2}} \arctan\left(\frac{u}{\sqrt{a}}\right), \tag{A8}$$

$$f_3(x,u) = \frac{1}{b}\ln\left(\frac{u^2/g^2}{u^2+b}\right) - \frac{1}{a}\ln\left(\frac{u^2/g^2}{u^2+a}\right). \tag{A9}$$

[1] N. Aghanim *et al.* (Planck Collaboration), Astron. Astrophys. **641**, A6 (2020); **652**, C4(E) (2021).
[2] G. B. Gelmini, in *Journeys Through the Precision Frontier: Amplitudes for Colliders* (World Scientific, Singapore, 2015), pp. 559–616.
[3] L. Bergstrom, Ann. Phys. (Berlin) **524**, 479 (2012).
[4] G. Bertone, D. Hooper, and J. Silk, Phys. Rep. **405**, 279 (2005).
[5] C.-Y. Chen, J. Kozaczuk, and Y.-M. Zhong, J. High Energy Phys. 10 (2018) 154.
[6] A. Berlin, N. Blinov, G. Krnjaic, P. Schuster, and N. Toro, Phys. Rev. D **99**, 075001 (2019).
[7] P. Agrawal *et al.*, Eur. Phys. J. C **81**, 1015 (2021).
[8] B. Abi *et al.* (Muon g-2 Collaboration), Phys. Rev. Lett. **126**, 141801 (2021).
[9] T. Aoyama *et al.*, Phys. Rep. **887**, 1 (2020).
[10] G. W. Bennett *et al.* (Muon g-2 Collaboration), Phys. Rev. D **73**, 072003 (2006).
[11] S. Borsanyi *et al.*, Nature (London) **593**, 51 (2021).
[12] M. Cè *et al.*, Phys. Rev. D **106**, 114502 (2022).
[13] T. Blum *et al.*, arXiv:2301.08696.
[14] A. Bazavov *et al.*, Phys. Rev. D **107**, 114514 (2023).
[15] C. Alexandrou, S. Bacchio, P. Dimopoulos, J. Finkenrath, R. Frezzotti, G. Gagliardi *et al.* (Extended Twisted Mass Collaboration), Phys. Rev. D **107**, 074506 (2023).
[16] T. Blum, P. A. Boyle, V. Gülpers, T. Izubuchi, L. Jin, C. Jung, A. Jüttner, C. Lehner, A. Portelli, and J. T. Tsang (RBC, UKQCD Collaborations), Phys. Rev. Lett. **121**, 022003 (2018).
[17] H. Wittig, Progress on $(g-2)_\mu$ on lattice QCD, *Presentation at the 57th Rencontres de Moriond EW 2023, La Thuile* (2023).
[18] F. V. Ignatov *et al.* (CMD-3 Collaboration), arXiv:2302.08834.
[19] Y. Kahn, G. Krnjaic, N. Tran, and A. Whitbeck, J. High Energy Phys. 09 (2018) 153.
[20] C.-Y. Chen, M. Pospelov, and Y.-M. Zhong, Phys. Rev. D **95**, 115005 (2017).
[21] D. V. Kirpichnikov, H. Sieber, L. Molina Bueno, P. Crivelli, and M. M. Kirsanov, Phys. Rev. D **104**, 076012 (2021).
[22] H. Sieber, D. Banerjee, P. Crivelli, E. Depero, S. N. Gninenko, D. V. Kirpichnikov, M. M. Kirsanov, V. Poliakov, and L. M. Bueno, Phys. Rev. D **105**, 052006 (2022).
[23] S. Gninenko (NA64 Collaboration), Addendum to the Proposal P348: Search for dark sector particles weakly coupled to muon with NA64μ, Technical Report, CERN, Geneva, 2018.
[24] E. Cortina Gil *et al.* (NA62 Collaboration), J. High Energy Phys. 11 (2022) 011.
[25] C. Rella, B. Döbrich, and T.-T. Yu, Phys. Rev. D **106**, 035023 (2022).
[26] E. Cortina Gil *et al.* (HIKE Collaboration), arXiv:2211.16586.
[27] M. Alviggi *et al.*, SHADOWS search for hidden and dark objects with the SPS, Report No. CERN-SPSC-2022-030/SPSC-I-256, 2022.
[28] K. Asai, T. Moroi, and A. Niki, Phys. Lett. B **818**, 136374 (2021).
[29] K. Asai, S. Iwamoto, M. Perelstein, Y. Sakaki, and D. Ueda, arXiv:2301.03816.
[30] C. Cesarotti, S. Homiller, R. K. Mishra, and M. Reece, Phys. Rev. Lett. **130**, 071803 (2023).
[31] G. Grilli di Cortona and E. Nardi, Phys. Rev. D **105**, L111701 (2022).
[32] B. Abi *et al.* (DUNE Collaboration), arXiv:2002.03005.
[33] M. Bondi, A. Celentano, R. R. Dusaev, D. V. Kirpichnikov, M. M. Kirsanov, N. V. Krasnikov, L. Marsicano, and D. Shchukin, Comput. Phys. Commun. **269**, 108129 (2021).
[34] M. Kirsanov, J. Phys. Conf. Ser. **2438**, 012085 (2023).
[35] B. Batell, N. Lange, D. McKeen, M. Pospelov, and A. Ritz, Phys. Rev. D **95**, 075003 (2017).
[36] K. Cheung, J.-L. Kuo, P.-Y. Tseng, and Z. S. Wang, Phys. Rev. D **106**, 095029 (2022).
[37] C.-Y. Chen, H. Davoudiasl, W. J. Marciano, and C. Zhang, Phys. Rev. D **93**, 035006 (2016).
[38] J. P. Leveille, Nucl. Phys. **B137**, 63 (1978).
[39] M. Lindner, M. Platscher, and F. S. Queiroz, Phys. Rep. **731**, 1 (2018).
[40] D. V. Kirpichnikov, V. E. Lyubovitskij, and A. S. Zhevlakov, Phys. Rev. D **102**, 095024 (2020).
[41] T. Moroi and A. Niki, J. High Energy Phys. 05 (2023) 016.
[42] D. Forbes, C. Herwig, Y. Kahn, G. Krnjaic, C. Mantilla Suarez, N. Tran, and A. Whitbeck, Phys. Rev. D **107**, 116026 (2023).
[43] R. Balkin, C. Delaunay, M. Geller, E. Kajomovitz, G. Perez, Y. Shpilman, and Y. Soreq, Phys. Rev. D **104**, 053009 (2021).
[44] Y.-S. Liu, D. McKeen, and G. A. Miller, Phys. Rev. D **95**, 036010 (2017).
[45] S. N. Gninenko, D. V. Kirpichnikov, M. M. Kirsanov, and N. V. Krasnikov, Phys. Lett. B **782**, 406 (2018).
[46] Y.-S. Liu and G. A. Miller, Phys. Rev. D **96**, 016004 (2017).

[47] R. Mertig, M. Bohm, and A. Denner, Comput. Phys. Commun. **64**, 345 (1991).
[48] Wolfram Research, Inc., Mathematica, Version 13.1, Champaign, IL, 2022.
[49] K. J. Kim and Y.-S. Tsai, Phys. Rev. D **8**, 3109 (1973).
[50] J. Alwall, R. Frederix, S. Frixione, V. Hirschi, F. Maltoni, O. Mattelaer, H. S. Shao, T. Stelzer, P. Torrielli, and M. Zaro, J. High Energy Phys. 07 (2014) 079.
[51] A. Belyaev, N. D. Christensen, and A. Pukhov, Comput. Phys. Commun. **184**, 1729 (2013).
[52] L. Marsicano, M. Battaglieri, A. Celentano, R. De Vita, and Y.-M. Zhong, Phys. Rev. D **98**, 115022 (2018).
[53] A. S. Zhevlakov, D. V. Kirpichnikov, and V. E. Lyubovitskij, Phys. Rev. D **106**, 035018 (2022).
[54] T. Eichlersmith, J. Mans, O. Moreno, J. Muse, M. Revering, and N. Toro, Comput. Phys. Commun. **287**, 108690 (2023).
[55] N. Arefyeva, S. Gninenko, D. Gorbunov, and D. Kirpichnikov, Phys. Rev. D **106**, 035029 (2022).
[56] A. Ariga, R. Balkin, I. Galon, E. Kajomovitz, and Y. Soreq, arXiv:2305.03102.
[57] H. Davoudiasl, R. Marcarelli, and E. T. Neil, J. High Energy Phys. 02 (2023) 071.
[58] M. Galassi *et al.*, GNU Scientific Library Reference Manual (2018).
[59] S. Agostinelli *et al.* (Geant4 Collaboration), Nucl. Instrum. Methods Phys. Res., Sect. A **506**, 250 (2003).
[60] I. Galon, E. Kajamovitz, D. Shih, Y. Soreq, and S. Tarem, Phys. Rev. D **101**, 011701(R) (2020).